Revista Brasileira de Física Médica.2011;5(1):89-92.

Influence of brain region of interest location for apparent diffusion coefficient maps calculation for reference values to be used in the in vivo characterization of brain tumors in magnetic resonance images

Influência da localização da região de interesse cerebral para cálculo dos mapas do coeficiente de difusão aparente para valores de referência a serem utilizados na caracterização in vivo de imagens de ressonância magnética de tumores cerebrais

Edna M. Souza[1,2,3], Gabriela Castellano[3,4] and Eduardo T. Costa[1,2]

[1]Center of Biomedical Engineering of the State University of Campinas (UNICAMP) - Campinas (SP), Brazil.
[2]Biomedical Engineering Department of Electrical and Computational Engineering School of UNICAMP - Campinas (SP), Brazil.
[3]Neurophysics Group, Cosmic Rays and Cronology Department, Gleb Wataghin Physics Institute, UNICAMP - Campinas (SP), Brazil.
[4]ClnAPCe Program (Cooperação Interinstitucional de Apoio a Pesquisas sobre o Cérebro) - São Paulo (SP), Brazil.

Abstract

In general, pathologic processes, such as neoplasic cell changes, tend to alter the magnitude of structural organization by destruction or reorganization of membranous elements or by a change in cellularity. These changes will also have an impact on proton mobility, which can be followed up by DWI (diffusion weighted magnetic resonance imaging). From DWI is obtained the ADC (apparent diffusion coefficient) map, which is a representation of the magnitude of water diffusion at the points of a given region of interest (ROI). The purpose of this study was to assess the variation of ADC values in different brain ROIs of normal subjects, using a computer tool previously developed. The aim of this assessment was to verify whether ADC values could be used to differentiate between normal subjects and patients with multiform glioblastoma (a high-grade glioma) and meningioma. ADC maps were calculated for 10 controls, 10 patients with glioblastoma and 10 with meningioma. For controls, mean ADC values were calculated for 10 different ROIs, located in the same places where the tumors were present in the patients. These values were then averaged over ROIs and over subjects, giving a mean ADC value of $(8.65\pm0.98)\times10^{-4}$ mm^2/s. The mean ADC values found for brain tumors were $(5.03\pm0.67)\times10^{-4}$ mm^2/s for meningioma and $(2.83\pm0.45)\times10^{-4}$ mm^2/s for glioblastoma. We concluded that the ROIs used for computing brain ADC values for controls were not essential for the estimation of normal reference ADC values to be used in the differentiation between these types of tumors and healthy brain tissue.

Keywords: magnetic resonance, diffusion, brain tumors, computer-assisted image processing.

Resumo

Em geral, os processos patológicos, como as alterações celulares neoplásicas, tendem a alterar a magnitude da organização estrutural pela destruição ou reorganização dos elementos membranosos, ou pela mudança na celularidade. Tais mudanças também terão um impacto na mobilidade do próton, que pode ser acompanhada pela imagem ponderada de difusão. Pela imagem ponderada de difusão, pode-se obter o mapeamento do coeficiente de difusão aparente, que é a representação da magnitude da difusão da água nos pontos de certa região de interesse. O objetivo deste estudo foi avaliar a variação dos valores do coeficiente de difusão aparente em diferentes regiões de interesse cerebral de indivíduos normais, utilizando uma ferramenta computacional que foi previamente desenvolvida. O objetivo desta avaliação foi verificar se os valores do coeficiente de difusão aparente poderiam ser utilizados para diferenciar indivíduos normais de pacientes com glioblastoma multiforme (um glioma de alto grau) e meningioma. Os mapeamentos do coeficiente de difusão aparente foram calculados para dez controles, dez pacientes com glioblastoma e dez com meningioma. Para os controles, os valores do coeficiente de difusão aparente médio foram calculados para dez diferentes regiões de interesse, localizadas nos mesmos lugares onde os tumores estavam presentes nos pacientes. Esses valores foram, em seguida, calculados sobre as regiões de interesse e sobre os sujeitos, fornecendo um valor do coeficiente de difusão aparente médio de $(8,65\pm0,98)\times10^{-4}$ mm^2/s. Os valores médios do coeficiente de difusão aparente encontrados para tumores cerebrais foram de $(5,03\pm0,67)\times10^{-4}$ mm^2/s, para o meningioma, e $(2,83\pm0,45)\times10^{-4}$ mm^2/s, para o glioblastoma. Concluiu-se que as regiões de interesse utilizadas para se computar os valores do coeficiente de difusão aparente cerebral para os controles não foram essenciais para estimar os valores de referência normal, que deverão ser usados na diferenciação entre esses tipos de tumores e tecido cerebral saudável.

Palavras-chave: ressonância magnética, difusão, neoplasias encefálicas, processamento de imagem assistida por computador.

Corresponding author: Edna Marina de Souza – Cidade Universitária Zeferino Vaz, Center of Biomedical Engineering, UNICAMP – Barão Geraldo – CEP: 13.083-970 – Campinas (SP), Brazil – E-mail: emarina@ceb.unicamp.br

Introduction

In diffusion-weighted magnetic resonance imaging (DWI), the contrast is determined by the microscopic and random motion of water protons. In general, pathologic processes, such as neoplasic cell changes, tend to alter the structural organization of membranous elements through changes in cellularity[1]. Such changes affect the average trajectory of water molecules through tissue, which can be analyzed qualitatively and quantitatively using DWI. Based on these images and on T2 weighted images, ADC (Apparent Diffusion Coefficient) maps are calculated, whose values can be used to distinguish between normal and pathological brain tissue.

DWI can be obtained by pulse sequences commonly used for the acquisition of structural images with the insertion, in these sequences, of two gradients of equal magnitude and opposite orientations (or same orientation, but separated by a radiofrequency pulse of 180º), as shown as in Figure 1[2]. Thus, water protons that moved between the applications of both diffusion gradients will generate signals of different magnitudes, being of lower amplitude the signal from the instant after the last application of diffusion gradient. Figure 1 shows a Spin-Echo (SE) pulse sequence, commonly used to acquire diffusion images.

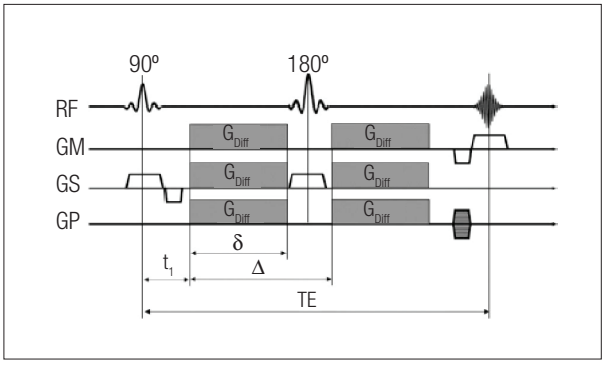

Figure 1. Spin-Echo (SE) pulse sequence for acquisition of DWI. (RF: radiofrequency pulse; GS: slice selection direction; GP: phase codification direction; GM: frequency codification direction. G_{diff}: diffusion gradient; t1: time between application of first RF pulse and first diffusion gradient; Δ: time between two diffusion gradients; δ: application time of diffusion gradient; TE: echo time).

Materials and methods

To develop the present study, DWI and T2 images present in a database of the Neuroimaging Laboratory, in UNICAMP hospital, were used. We analyzed 10 control subjects aged between 22 and 48 years (mean = 33.5 ± 3.8 years, 40% women), 10 patients with multiform glioblastoma aged between 42 and 64 years (mean = 49.6 ± 4.5 years, 40% women), and 10 patients with meningioma aged between 36 and 54 years (mean = 42.5 ± 2.8 years, 60% women). All tumor cases were confirmed by histopathological analysis performed after images acquisitions. The study was approved by the Ethics Review Board of UNICAMP Medical Sciences School. DWI and T2-weighted images were acquired in DICOM format in a Prestige 2T scanner, manufactured by Elscint (Haifa, Israel). Diffusion images were registered on T2 images using Mutual Information Maximization (MIM) and Affine Transformations (AT)[3]. This step was aimed at aligning DWI and T2 images, since despite these are acquired one after another, small head displacements along the scan result in voxel shift between the images. The ADC maps are calculated using a computational tool developed previously in Matlab®. From the DWI acquired in the x, y and z directions, a mean DW image (SI) was calculated, containing information about water diffusion. The SI image is given by:

$$SI = (SI_x SI_y SI_z)^{1/3} \quad (1)$$

SI_x, SI_y and SI_z are the DW images acquired along the x, y and z directions. The calculation of ADC values is performed using the following equation:

$$SI = SI_0 \times e^{-bADC} \quad (2)$$

SI_0 is the intensity of the T2 image, SI is the intensity of the diffusion-weighted image, b is the coefficient of diffusion sensitization in s/mm^2 and ADC is the ADC value, in mm^2/s. In the MRI scanner used, the parameter b was fixed to a value of 700 s/mm^2.

In order to facilitate the calculations and minimize noise in the ADC maps, a mask was developed in Matlab, using the Mathematical Morphology operations of dilation and closing, with a structuring element type diamond[4]. This mask allowed the application of the presented equations only on the places of the image corresponding to brain. ADC maps obtained were converted into DICOM images, and the ADC mean value in regions of interest (ROIs) corresponding to normal brain tissue and tumors were calculated and compared among themselves and with literature values. The ROIs were drawn using the software ImageJ® with guidance of a neurosurgeon, based on visual aspects of the tumor on the ADC map and considering its possible proliferation pathways.

To evaluate the possible existence of dependence between the ADC values and the brain region, mean ADC values were calculated on controls for 20 different ROIs located in the same places where the tumors (10 meningiomas and 10 glioblastomas) were present in the patients. These values were then averaged over ROIs and over subjects, giving a mean ADC value used as reference.

Results

Figure 2 shows examples of ADC maps calculated for a control subject and a patient with glioblastoma. The white ROI corresponds to the area of mean ADC calculation in tumor. Figure 3 shows examples of ADC maps calculated for a control subject and a patient with meningioma. The white ROI corresponds to the area of mean ADC calculation in tumor. Figure 4 shows a plot of mean ADC values for control subjects, patients with glioblastoma and patients with meningioma. Figure 5 shows the distribution of mean ADC values for control subjects obtained in ROIs of glioblastomas. Figure 6 shows mean ADC values for the control group in ROIs of glioblastoma excluding lateral ventricles. Figure 7 shows the distribution of mean ADC values for control subjects obtained in ROIs of meningioma.

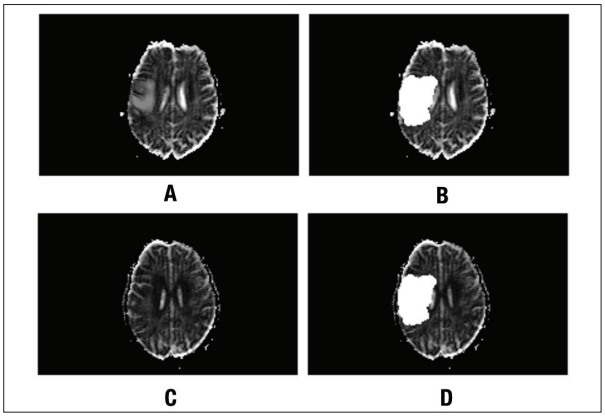

Figure 2. (A) ADC map for a patient with glioblastoma. (B) ROI for mean ADC calculation in tumor. (C) ADC map for a control subject. (D) Same (B) ROI applied to (C) ADC map for calculation of mean ADC values in healthy brain tissue located in the same place where the tumor was present in the patient.

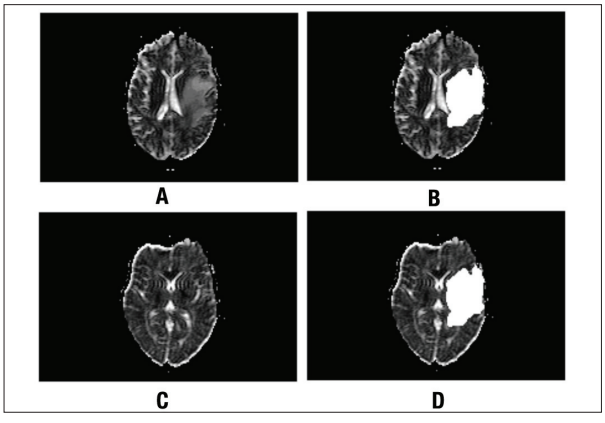

Figure 3. (A) ADC map for a patient with meningioma. (B) ROI for mean ADC calculation in tumor. (C) ADC map for a control subject. (D) Same (B) ROI applied to (C) ADC map for calculation of mean ADC values in healthy brain tissue located in the same place where the tumor was present in the patient.

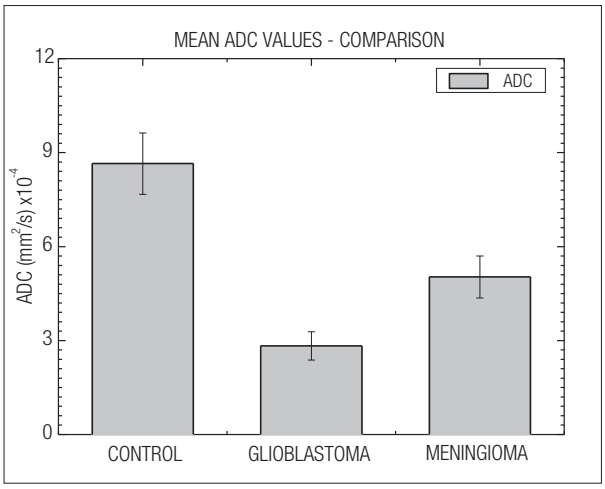

Figure 4. Mean ADC values for control group ((8.65±0.98) $\times 10^{-4}$ mm^2/s), glioblastoma patients ((2.83±0.45) $\times 10^{-4}$ mm^2/s), and meningioma patients ((5.03±0.67) $\times 10^{-4}$ mm^2/s).

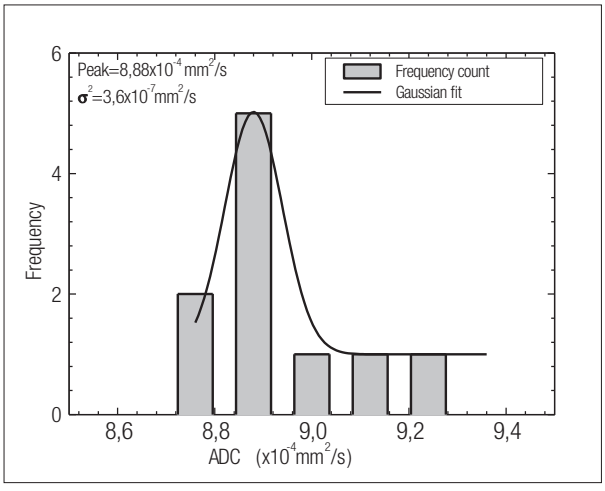

Figure 5. Distribution of mean ADC values for control group healthy brain tissue using the same ROIs used for mean ADC calculation in glioblastoma.

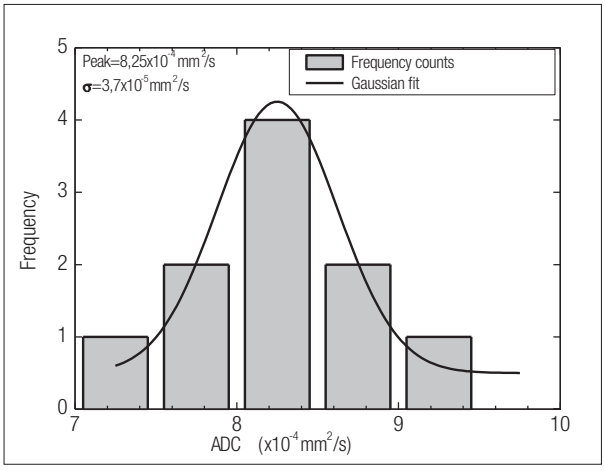

Figure 6. Distribution of mean ADC values for control group healthy brain tissue using the same ROIs used for mean ADC calculation in glioblastoma excluding the ROI portion that corresponds to the lateral ventricles.

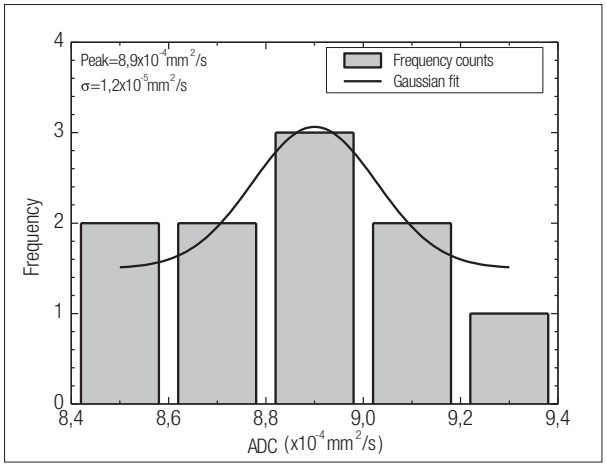

Figure 7. Distribution of mean ADC values for control group healthy brain tissue using the same ROIs used for mean ADC calculation in meningioma.

Discussion

For control subjects, patients with glioblastoma and patients with meningioma, the mean ADC values were (8.65 ± 0.98)×10^{-4} mm^2/s, (2.83 ± 0.45)×10^{-4} mm^2/s and (5.03 ± 0.67)×10^{-4} respectively, as seen in the graph of Figure 4. A t-test applied to the ADC values showed that they were significantly different ($p < 0.001$) between the groups of patients compared to healthy subjects. For glioblastoma, the values obtained agree with information found in the literature[5]. For control subjects, the value corresponds to regions containing normal white and gray matter[6].

The results found show that there is no significant influence of ROI location in the determination of ADC values for normal brain tissue in the control group. Moreover, it is possible to differentiate between healthy and tumoral brain tissue using ADC values. The protocol developed in this work should be further associated with other techniques of image processing, among which texture analysis tools that apply second-order statistics, such as co-occurrence and run length matrices. The calculation of ADC values for normal brain tissue using the same ROIs as in the group of tumors showed no significant dependency of ADC values of normal tissues with the brain region, as shown by the graphs of Figures 5-7. However, ROIs portions that overlap the lateral ventricles should be excluded from the calculation, since in those regions ADC values are much higher due to the flow of cerebrospinal fluid (CSF). The non-exclusion of the lateral ventricles from these calculations makes the distribution of ADC values show a tendency to higher values than those found in areas where there is only gray and white matter (Figure 5). In Figure 6, there is not this tendency. For meningioma, it is not necessary to exclude the lateral ventricles from the ADC calculation.

Glioblastoma are tumors of high cellularity[6]. The large concentration of tumor cells in a given region hinder the flow of water molecules through it, resulting in lower ADC values compared to the control condition.

Conclusion

Based on these results, it appears that the calculation of ADC values can be a useful tool for distinguishing between normal brain tissue and tumor.

Moreover, this tool should be associated with other techniques of image processing, such as co-occurrence and run-length matrices[7], taking into account the neighborhood relations between pixels in a given ROI in an attempt to obtain a computational resource that allows the characterization of healthy and pathological brain tissues noninvasively and in vivo in routine clinical practice.

References

1. Weiss TF. Cellular Biophysics, v. 1: Transport. Cambridge: Oxford Publishing Group; 2004.
2. Mansfield P. Multiplanar imaging formation using NMR spin-echoes. Solid State Physics. 1977;10:55-8.
3. Quasi AA. Image Registration Toolkit. Department of Computer Science, Copenhagen University; 2008.
4. Lotufo RA, Dougherty ER. Hands-on morphological image processing. Bellingham: SPIE Press; 2003.
5. Norris DG. The effects of microscopic tissue parameters on the diffusion weighted magnetic resonance imaging experiment. NMR Biomed. 2001;14(2):77-93.
6. Beaulileu C, Allen PS. Determinants of anisotropic water diffusion in nerves. Magn Reson Med. 1994;31(4):394-400.
7. Haralick RM. Statistical and structural approaches to texture. Proceedings of IEEE. 1979;67:786 -804.